PCCP

Accepted Manuscript




ROYAL SOCIETY OF CHEMISTRY

www.rsc.org/pccp

# ABSTRACT

The fragmentation products of the ε-carbon–centered radical cations $[\mathbf{Y}^{\boldsymbol{\varepsilon\bullet}}\mathrm{LG}]^+$ and $[\mathbf{Y}^{\boldsymbol{\varepsilon\bullet}}\mathrm{GL}]^+$, made by 266-nm laser photolysis of protonated 3-iodotyrosine-containing peptides, are substantially different from those of their π-centered isomers $[\mathbf{Y}^{\boldsymbol{\pi\bullet}}\mathrm{LG}]^+$ and $[\mathbf{Y}^{\boldsymbol{\pi\bullet}}\mathrm{GL}]^+$, made by dissociative electron transfer from a ternary metal–ligand–peptide complexes. For leucine-containing peptides the major pathway for the ε-carbon–centered radical cations is loss of the side chain of the leucine residue forming $[\mathrm{Y}\mathbf{G}^{\boldsymbol{\alpha\bullet}}\mathrm{G}]^+$ and $[\mathrm{YG}\mathbf{G}^{\boldsymbol{\alpha\bullet}}]^+$, whereas for the π-radicals it is the side chain of the tyrosine residue that is lost, giving $[\mathbf{G}^{\boldsymbol{\alpha\bullet}}\mathrm{LG}]^+$ and $[\mathbf{G}^{\boldsymbol{\alpha\bullet}}\mathrm{GL}]^+$. The fragmentations of the product ions $[\mathrm{Y}\mathbf{G}^{\boldsymbol{\alpha\bullet}}\mathrm{G}]^+$ and $[\mathrm{YG}\mathbf{G}^{\boldsymbol{\alpha\bullet}}]^+$ are compared with those of the isomeric $[\mathbf{Y}^{\boldsymbol{\varepsilon\bullet}}\mathrm{GG}]^+$ and $[\mathbf{Y}^{\boldsymbol{\pi\bullet}}\mathrm{GG}]^+$ ions. The collision-induced spectra of ions $[\mathbf{Y}^{\boldsymbol{\varepsilon\bullet}}\mathrm{GG}]^+$ and $[\mathrm{YG}\mathbf{G}^{\boldsymbol{\alpha\bullet}}]^+$ are identical, showing that interconversion occurs prior to dissociation. For ions $[\mathbf{Y}^{\boldsymbol{\varepsilon\bullet}}\mathrm{GG}]^+$, $[\mathbf{Y}^{\boldsymbol{\pi\bullet}}\mathrm{GG}]^+$ and $[\mathrm{Y}\mathbf{G}^{\boldsymbol{\alpha\bullet}}\mathrm{G}]^+$ the dissociation products are all distinctly different, indicating that dissociation occurs more readily than isomerization. Density functional theory calculations at B3LYP/6-31++G(d,p) gave the relative enthalpies (in kcal mol $^{-1}$ at 0 K) of the five isomers to be $[\mathbf{Y}^{\boldsymbol{\varepsilon\bullet}}\mathrm{GG}]^+$ 0, $[\mathbf{Y}^{\boldsymbol{\pi\bullet}}\mathrm{GG}]^+$ -23.7, $[\mathrm{YG}\mathbf{G}^{\boldsymbol{\alpha\bullet}}]^+$ -28.7, $[\mathrm{Y}\mathbf{G}^{\boldsymbol{\alpha\bullet}}\mathrm{G}]^+$ -31.0 and $[\mathbf{Y}^{\boldsymbol{\alpha\bullet}}\mathrm{GG}]^+$ -38.5. Migration of an α-C–H atom from the terminal glycine residue to the ε-carbon–centered radical in the tyrosine residue, a 1-11 hydrogen atom shift, has a low barrier, 15.5 kcal mol$^{-1}$ above $[\mathbf{Y}^{\boldsymbol{\varepsilon\bullet}}\mathrm{GG}]^+$ By comparison, isomerization of $[\mathbf{Y}^{\boldsymbol{\varepsilon\bullet}}\mathrm{GG}]^+$ to $[\mathrm{Y}\mathbf{G}^{\boldsymbol{\alpha\bullet}}\mathrm{G}]^+$ by a 1-8 hydrogen atom migration from the α-C–H atom of the central glycine residue has a much higher barrier (50.6 kcal mol$^{-1}$); similarly conversion of $[\mathbf{Y}^{\boldsymbol{\varepsilon\bullet}}\mathrm{GG}]^+$ into $[\mathbf{Y}^{\boldsymbol{\pi\bullet}}\mathrm{GG}]^+$ has a higher energy (24.4 kcal mol$^{-1}$).

# Formation, Isomerization, and Dissociation of ε- and α-Carbon–Centered Tyrosylglycylglycine Radical Cations

Cheuk-Kuen Lai[1], Xiaoyan Mu[1], Qiang Hao[1], Alan C. Hopkinson[2,*] and Ivan K. Chu[1,*]

[1] Department of Chemistry, The University of Hong Kong, Hong Kong, China. Email: ivankchu@hku.hk

[2] Department of Chemistry and Centre for Research in Mass Spectrometry, York University, Toronto, Canada. Email: ach@yorku.ca

[*] Corresponding Author

## Table of content

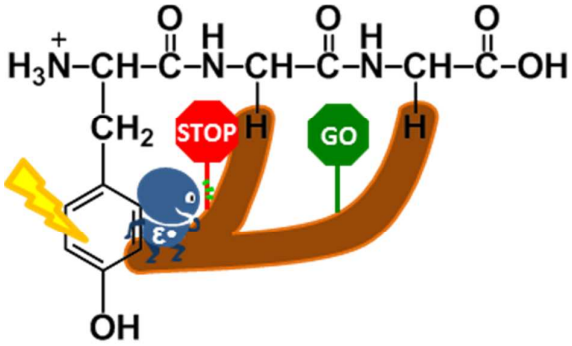

# INTRODUCTION

Odd-electron peptide radical ions exhibit complementary fragment information with respect to their even-electron protonated counterparts, potentially providing more complete sequencing information.[1-9] The locations of the radical center and the charge in a peptide radical cation govern how the peptide fragments within a mass spectrometer.[6, 10-12] Barriers to hydrogen atom transfer (HAT) are frequently lower than those to dissociation; consequently, the initially-formed ion may rearrange to an isomer prior to collision-induced dissociation (CID). Experimental investigations of the interconversion between isomers of peptide radical cations can begin with the experimental of radical cations involving ions with different well-defined initial radicals sites within the same peptide. A number of approaches can be used to generate these radicals.[10, 13-24] One frequently exploited method is through side-chain losses from peptide radical cations generated by electron transfer from metal–ligand–peptide complexes.[13] Here $C_\alpha$–$C_\beta$ bond cleavages of tryptophan and tyrosine residues can result in well-defined radical centers on the corresponding α-carbon atoms after neutral losses of 3-methylene-3*H*-indole (129 Da) or *p*-quinomethide (106 Da), respectively.[10, 13, 25, 26] Also, well-defined radical centers can be produced through low energy collision-induced dissociation (CID) of chemically modified amino acids; for example, reacting a tryptophan-containing peptide with sodium nitrite ($NaNO_2$) or *tert*-butylnitrite to produce N-nitrosylation[15] or a cysteine-containing peptide with *tert*-butylnitrite/*S*-nitrosoglutathione to give *S*-nitrosocysteine,[16, 17] followed by elimination of NO by CID to yield radicals initially located at the nitrogen and sulfur atoms respectively.[15-17] The Julian group has used various ultraviolet chromophores and a 266-nm laser to photochemically generate well-defined radicals from protonated peptides;[18-23] These include (1) Using a non-covalently bound complex between a

naphthyl based crown ether adduct and a lysine or arginine residue, to photoexcite the peptide;[18] (2) Replacing the phosphate group in peptides phosphorylated at serine or threonine residues by a covalently bound 2-naphthalenethiol and then using UV to homolytically cleave the C–S bond to create a β-radical;[19, 20] (3) For peptides that contain a disulfide bond, exciting the S–S bond which leads to homolytic cleavage of this bond forming thiol radicals;[21] and (4) Reaction of a tyrosine-containing peptide with sodium iodide and chloramine-T to form a 3-iodotyrosine residue followed by irradiation to cleave the weak C–I bond and formation of an $\sigma_\varepsilon$-radical.[22, 23]

In a previous study,[27] we observed both similarities and differences when comparing molecular radical cations ($M^{\bullet+}$) generated through 266-nm laser photolysis of iodotyrosine-containing peptides with those formed through dissociative electron transfer in ternary metal–ligand–peptide complexes. We suspected that these differences arose from substantial energy barriers restricting hydrogen atom migrations in non-basic peptide radical cations. For the $[YAGFLG]^{\bullet+}$ derived from metal–ligand–peptide complexes, we observed abundant tyrosine side-chain losses (*p*-cresol radical, $[H_2C^{\bullet}C_6H_4OH]$, 107 Da); by contrast, in the CID of the peptide radical generated by 266-nm laser photolysis, we observed abundant leucine side-chain losses (isopropyl radical, $[(CH_3)_2C^{\bullet}H]$, 43 Da; isobutene, $[H_2C{=}C(CH_3)_2]$, 56 Da) with very little tyrosine side-chain loss.[27] $C_\alpha$–$C_\beta$ Bond cleavage (loss of 56 Da) occurs from an ion in which the radical center is located on the γ-carbon atom of the leucine residue, while $C_\beta$–$C_\gamma$ bond cleavage (loss of 43 Da) occurs from the ion in which the radical is located on α-carbon atom.[28, 29] We expected loss of an iodine atom to generate a sigma epsilon ($\sigma_\varepsilon$) radical by homolytic cleavage of the C–I bond of the tyrosine ring; therefore, it appears that subsequent hydrogen atom migrations must have occurred from the leucine residue to the $\sigma_\varepsilon$ radical prior to the $C_\alpha$–$C_\beta$/$C_\beta$–$C_\gamma$ bond cleavages.

Here we use the model peptide radical cation $YGG^{\bullet+}$ to examine interconversion between the $\sigma_\varepsilon$ radical on the tyrosine residue, denoted $[\mathbf{Y}^{\varepsilon\bullet}GG]^+$, and isomers with the radical center on the α-carbons on the glycine residues. To generate the α-radicals $[Y\mathbf{G}^{\alpha\bullet}G]^+$ and $[YG\mathbf{G}^{\alpha\bullet}]^+$ we took advantage of our previous discovery that $\sigma_\varepsilon$ radicals on a tyrosine residue induce the loss of the entire side chain of an adjacent leucine residue as isobutene.[21]

# EXPERIMENTAL

## Materials and Reagents

Fmoc-Protected amino acids and Wang resin were purchased from Advanced ChemTech (Louisville, KY, USA). All of the studied peptides were synthesized according to procedures described in the literature.[30] All solvents were of HPLC grade; MeOH, $H_2O$, and AcOH were purchased from Duksan Pure Chemicals (Ansan-City, Gyungkido, Korea), Tedia (Fairfield, OH, USA), and VWR International (Poole, England), respectively. The tyrosine-containing peptides were iodinated according to a published protocol.[23] To prepare solutions of iodinated peptides, 1 mole equivalent of $NH_4I$ (instead of NaI, to avoid $Na^+$ counter ions) was added to a solution (1 mL) containing the peptide (0.1 mM) in $H_2O$/MeOH (50:50, v/v) and then chloramine-T (1 mole equivalent) was added; after 45 s, the reaction was quenched by adding sodium metabisulfite (1 mole equivalent).

## Mass Spectrometry

In a typical infusion experiment, a syringe pump (Cole Parmer, Vernon Hills, IL, USA) was used to deliver samples at a flow rate of 120 μL $h^{-1}$. The peptide stock solutions for experiments with singly protonated peptides containing iodine ($[M + I + H]^+$) typically comprised 0.1 mM peptide in $H_2O$/MeOH (50:50, v/v) containing 0.1% AcOH. When generating peptide radicals using metal complexes, 600 μM $Cu^{II}$(12-crown-4) was added to the peptide stock solutions, without AcOH, such that peptide radical ions ($M^{\bullet+}$) would be generated through one-electron transfer from the neutral peptide to the metal center in the metal–ligand–peptide complex during gas phase. All laser-induced dissociation (LID) and CID experiments were conducted using a modified triple quadrupole linear-ion trap (LIT) (QTRAP®, AB SCIEX,

Concord, ON, Canada) equipped with an electrospray ionization (ESI) source with +3500V and $N_2$ as the collision gas. The detailed setup for LID has been described previously;[27] briefly, a fourth-harmonic laser pulse, with a pulse width of 4 ns and a pulse energy of 3 mJ, was generated by a flashlamp-pumped Nd:YAG laser (Tempest 20, Electro Scientific Industries, Portland, OR, USA), which was triggered by the signal from the modified mass spectrometer. The $\sigma_\varepsilon$ radical cations $[\mathbf{Y}^{\varepsilon\bullet}\mathrm{LG}]^+$, and $[\mathbf{Y}^{\varepsilon\bullet}\mathrm{GL}]^+$ were generated through 266-nm laser photolysis, with loss of the iodine atom from the protonated 3-iodotyrosine-containing peptides of $[\mathrm{Y_I LG} + \mathrm{H}]^+$ and $[\mathrm{Y_I GL} + \mathrm{H}]^+$. The $\pi$ radical cations, $[\mathbf{Y}^{\pi\bullet}\mathrm{LG}]^+$ and $[\mathbf{Y}^{\pi\bullet}\mathrm{GL}]^+$, were produced through dissociative electron transfer in ternary metal–ligand–peptide complexes $[\mathrm{Cu(12\text{-}crown\text{-}4)(peptide)}]^{\bullet 2+}$ under low energy CID. The $\sigma_\alpha$ radical cation, $[\mathrm{Y}\mathbf{G}^{\alpha\bullet}\mathrm{G}]^+$ and $[\mathrm{YG}\mathbf{G}^{\alpha\bullet}]^+$, were generated by CID of $[\mathbf{Y}^{\varepsilon\bullet}\mathrm{LG}]^+$ and $[\mathbf{Y}^{\varepsilon\bullet}\mathrm{GL}]^+$ (**Figures 1a** and **1c**) which underwent facile diagnostic losses of neutral isobutene ($[\mathrm{CH_2{=}C(CH_3)_2}]$, 56 Da).

## Confirmation of Peak Assignment

The glycine on the C-terminus of YLG was replaced by alanine, such that the C-terminus fragment ions of $[\mathbf{Y}^{\varepsilon\bullet}\mathrm{LA}]^+$ (Supplementary Information, **Figure S1a**) would be mass-shifted by *m/z* +14 relative to those of $[\mathbf{Y}^{\varepsilon\bullet}\mathrm{LG}]^+$ while N-terminus fragments remain unchanged. Similarly, second amino acid residue in YGL was replaced by alanine so that N-terminus fragment ions of $[\mathbf{Y}^{\pi\bullet}\mathrm{AL}]^+$ (i.e. $b_2$-H and $[\mathrm{M\text{-}106}]^{\bullet+}$) would be mass-shifted by *m/z* +14 relative to those of $[\mathbf{Y}^{\pi\bullet}\mathrm{GL}]^+$.

## Computational Methods

All calculations were performed in the framework of density functional theory (DFT) using the unrestricted (U) hybrid functional formulated with a mixture of Hartree–

Fock exchange energy and Becke's three-parameter 1988 gradient-corrected exchange energy, as well as Lee–Yang–Parr (LYP) correlation energy (UB3LYP).[31] All DFT calculations were performed initially with the 6-31G basis set and subsequently with the 6-31++G(d,p) basis set.[32, 33] Low-lying structures of the molecular ions were initially obtained through Monte Carlo conformational searches with a semi-empirical method (PM3) using Spartan software;[34] the 200 most stable conformers in maximum were selected (i.e. all conformers are chosen for all molecular ions) for geometry optimization after the conformational search at the UB3LYP/6-31G and UB3LYP/6-31++G(d,p) levels. All of the stationary points were characterized by vibrational analysis to ensure that their curvatures were correct on the corresponding potential energy surfaces (PESs) and the intrinsic reaction coordinate (IRC) method was used to identify the local minima associated with each transition state structure. Relative enthalpies at 0 K ($\Delta H_0°$) were calculated from the electronic energies and zero-point energies (ZPVE) obtained within the harmonic approximation. Spin densities were obtained using natural population analysis (NPA). All DFT calculations were performed using the Gaussian 03 software package.[35]

The microcanonical rate constant $k_i(E)$ of each unimolecular reaction $i$ was calculated using the Rice–Ramsperger–Kassel–Marcus (RRKM) equation.[36] The value of $k_i(E)$ is a function of the internal energy $E$ of the reactant, relative to the energy of the structure at the global minimum on the PES; it is given by eq 1:

$$k_i(E) = \frac{\sigma W_i^{\ddagger}(E_i - E_{0i})}{h\rho_i(E_i)}$$

where $E_i = E - \Delta H_{0i}$ is the available vibrational energy ($\Delta H_{0i}$ is the $i^{th}$ reactant's enthalpy of formation at 0 K), $\rho_i(E_i)$ is the density of vibrational states of the reactant, $W_i^{+}$ $(E_i - E_{0i})$ is the sum of the vibrational states of the transition state, $E_{0i}$ is the corresponding critical energy for reaction, $h$ is Planck's constant, and σ is the reaction

path degeneracy (equal to 1 in all of the reaction pathways considered in this study). The vibrational states were counted directly using the Beyer–Swinehart algorithm.[37]

# RESULTS AND DISCUSSION

## Fragmentations of isomers of $[YLG]^{\bullet+}$ and $[YGL]^{\bullet+}$

**Figures 1a** and **1b** display the CID spectra of isomeric tripeptides of tyrosylleucylglycine, $[YLG]^{\bullet+}$, with different initial radical sites; these radical cations were generated using two different methods (**Scheme 1**). The $\sigma_\varepsilon$ radical $[\mathbf{Y}^{\varepsilon\bullet}\mathrm{LG}]^+$, formed through 266-nm laser photolysis of the 3-iodotyrosine-containing peptide $[\mathbf{Y_I}\mathrm{LG} + \mathrm{H}]^+$, has a well-defined initial ε-carbon–centered radical on the tyrosine residue. Spectrum **1b** is for the π radical $[\mathbf{Y}^{\pi\bullet}\mathrm{LG}]^+$ formed through dissociative electron transfer from a ternary metal–ligand–peptide complex. These product ion spectra of isomeric $[\mathbf{Y}^{\varepsilon\bullet}\mathrm{LG}]^+$ and $[\mathbf{Y}^{\pi\bullet}\mathrm{LG}]^+$ are strikingly different: the former underwent $C_\alpha$–$C_\beta$ cleavage of the leucine residue ($[M - 56]^{\bullet+}$) to generate the $\sigma_\alpha$ radical[28] $[\mathrm{Y}\mathbf{G}^{\alpha\bullet}\mathrm{G}]^+$ (**Scheme 1c**), as well as some other fragment ions in lower abundance ($[M - 17]^{\bullet+}$, $[b_2 - H - 17]^{\bullet+}$, $[c_1 - 17]^+$); the latter underwent $C_\alpha$–$C_\beta$ cleavage of the tyrosine residue (forming $[M - 106]^{\bullet+}$) after proton abstraction from the phenolic oxygen atom and also formed $[M - 17]^{\bullet+}$ and $[b_2 - H]^{\bullet+}$ ions in lower abundance. Assignments were verified by corresponding studies of the radical peptide analogues $[\mathbf{Y}^{\varepsilon\bullet}\mathrm{LA}]^+$ and $[\mathbf{Y}^{\pi\bullet}\mathrm{LA}]^+$, which differ from $[\mathbf{Y}^{\varepsilon\bullet}\mathrm{LG}]$ and $[\mathbf{Y}^{\varepsilon\bullet}\mathrm{LG}]^+$ by replacing the terminal glycine residue with an alanine residue (see **Figures S1a–d** in the Supplementary Information and the discussion in the Experimental section). The observation of distinctly different product ion spectra for $[\mathbf{Y}^{\varepsilon\bullet}\mathrm{LG}]^+$ and $[\mathbf{Y}^{\pi\bullet}\mathrm{LG}]^+$ was not unexpected; it is in accordance with recent results[27] from longer isomeric peptides with initial ε-carbon– and π-centered radicals at the tyrosine residue. In summary, the major fragmentation pathways for $\sigma_\varepsilon$ and $\sigma_\alpha$ radical cations are different indicating that the barriers to fragmentation are lower than those to isomerization. For $[\mathbf{Y}^{\varepsilon\bullet}\mathrm{LG}]^+$, hydrogen atom transfer from the γ-carbon of the leucine residue to the radical center

on the aromatic ring precedes the loss of isobutene and for $[\mathbf{Y}^{\boldsymbol{\pi\bullet}}\mathrm{LG}]^+$ proton transfer from the OH of the tyrosine residue to the backbone is followed by loss of *p*-quinomethide.

**Figures 1c and 1d** present CID spectra of isomers $[\mathbf{Y}^{\boldsymbol{\varepsilon\bullet}}\mathrm{GL}]^+$ and $[\mathbf{Y}^{\boldsymbol{\pi\bullet}}\mathrm{GL}]^+$. The fragmentation patterns of the π-radical system $[\mathbf{Y}^{\boldsymbol{\pi\bullet}}\mathrm{LG}]^+$ is very similar to that of $[\mathbf{Y}^{\boldsymbol{\pi\bullet}}\mathrm{GL}]^+$, although the latter has additional products $[b_2 - H - 17]^{\bullet+}$ and $[c_1 - 17]^+$ albeit in low abundance. However, there is a substantial difference in the spectra of the $\sigma_\varepsilon$ radical isomers $[\mathbf{Y}^{\boldsymbol{\varepsilon\bullet}}\mathrm{LG}]^+$ and $[\mathbf{Y}^{\boldsymbol{\varepsilon\bullet}}\mathrm{GL}]^+$. In addition to formation of the $[M - 56]^{\bullet+}$ radical cation by $C_\alpha$–$C_\beta$ cleavage of the leucine residue initiated by HAT from the γ-carbon to the ε-carbon, an $[M - 43]^+$ ion was also observed in low abundance; the latter is the product of $C_\beta$–$C_\gamma$ bond cleavage of the leucine side chain and is the result of HAT to the ε-carbon–centered radical from the α-carbon of the leucine residue. Similarly we observed a (–29 Da) loss resulting from $C_\beta$–$C_\gamma$ bond cleavage of $[\mathbf{Y}^{\boldsymbol{\varepsilon\bullet}}\mathrm{GI}]^+$ (Supplementary Information, **Figure S1e**), in which an isoleucine residue replaced the third leucine residue.

Previous explorations of tautomerizations among α-carbon atoms along a peptide backbone or between α-carbon– and π-centered radicals have revealed that rearrangements are energetically and kinetically hindered by the presence of the charge on the backbone.[10] Hydrogen atom migration along the backbone can be facilitated by the presence of a basic amino acid residue that sequesters the proton.[10, 38] To the best of our knowledge, relatively little is known about the mechanism for hydrogen atom transfers between ε-carbon–centered ($\sigma_\varepsilon$) radicals and α-carbon–centered radicals ($\sigma_\alpha$), although they apparently have a substantial impact on the ion-fragmentation chemistry.[39, 40] Accordingly, here we present a combined experimental and theoretical investigation of three simple isomeric radical cations of tyrosylglycylglycine: $[\mathbf{Y}^{\boldsymbol{\varepsilon\bullet}}\mathrm{GG}]^+$, with the radical centered at the ε-carbon atom at the

ortho position of the phenolic unit, and $[Y\mathbf{G}^{\alpha\bullet}G]^+$ and $[YG\mathbf{G}^{\alpha\bullet}]^+$, where the radicals are centered at the α-carbon atoms of the second and third glycine residues, respectively. This tyrosine-containing prototypical system allows us to explore how interconversions associated with the ε- and α-carbon–centered radicals along the peptide backbone influence their subsequent dissociation processes.

## Interconversion of radical cations of YGG

**Figure 2** presents the CID spectra of $[\mathbf{Y}^{\varepsilon\bullet}GG]^+$, $[Y\mathbf{G}^{\alpha\bullet}G]^+$ and $[YG\mathbf{G}^{\alpha\bullet}]^+$. The CID spectra of $[\mathbf{Y}^{\varepsilon\bullet}GG]^+$ and $[YG\mathbf{G}^{\alpha\bullet}]^+$ are almost identical whereas that for $[Y\mathbf{G}^{\alpha\bullet}G]^+$ is simpler and very different (mass assignments verified in Supplementary Information, **Figure S3**). All three spectra have $[b_2 - H - 17]^{\bullet+}$ and $[c_1 - 17]^+$ ions, but for $[Y\mathbf{G}^{\alpha\bullet}G]^+$ the only other product is the ion at *m/z* 278 (loss of $NH_3$), an ion in negligible abundance in the other two spectra. The base peak for $[\mathbf{Y}^{\varepsilon\bullet}GG]^+$, and $[YG\mathbf{G}^{\alpha\bullet}]^+$ is a result of the loss of water and, on further dissociation, the product $[M - 18]^{\bullet+}$ ion does not lose CO, indicating that it is not an oxazolone (see Supplementary **Figure S2**). From this we conclude that the oxygen eliminated probably originates in an amide group.[41, 42] Additional products from $[\mathbf{Y}^{\varepsilon\bullet}GG]^+$, and $[YG\mathbf{G}^{\alpha\bullet}]^+$ are the $a_1^+$ ion in high abundance with $b_2^+$, $[b_2 + H - 17]^{\bullet+}$ and $[M - 106]^{\bullet+}$ ions all in moderate abundance. Here we note that both experimental and theoretical studies on the three carbon-centered $[\mathbf{G}^{\alpha\bullet}GG]^+$, $[G\mathbf{G}^{\alpha\bullet}G]^+$ and $[GG\mathbf{G}^{\alpha\bullet}]^+$ radical cations revealed that only the $[GG\mathbf{G}^{\alpha\bullet}]^+$ species generates the closed-shell even-electron $b_2^+$ ion and its complementary neutral radical $[Gly\text{-}H]^\bullet$; in other words, the formation of the $b_2^+$ ion necessitated formation of a $[GG\mathbf{G}^{\alpha\bullet}]^+$.[43] The presence of a $b_2^+$ ion in the spectra of both $[\mathbf{Y}^{\varepsilon\bullet}GG]^+$ and $[YG\mathbf{G}^{\alpha\bullet}]^+$ then provides further evidence for tautomerization between $[\mathbf{Y}^{\varepsilon\bullet}GG]^+$ and $[YG\mathbf{G}^{\alpha\bullet}]^+$. These results clearly suggest that the $[\mathbf{Y}^{\varepsilon\bullet}GG]^+$ and $[YG\mathbf{G}^{\alpha\bullet}]^+$ ions interconvert prior to dissociation and that the $[Y\mathbf{G}^{\alpha\bullet}G]^+$ dissociates

more readily than convert into the other two structures.

DFT calculations have been used to examine pathways to interconversions between the $\sigma_\varepsilon$ and $\sigma_\alpha$ radical cationic tripeptides of $[\mathbf{Y}^{\varepsilon\bullet}GG]^+$, $[Y\mathbf{G}^{\alpha\bullet}G]^+$, and $[YG\mathbf{G}^{\alpha\bullet}]^+$. **Figure 3** displays the spin densities of the $\sigma_\varepsilon$ radical $[\mathbf{Y}^{\varepsilon\bullet}GG]^+$, the $\pi$ radical $[\mathbf{Y}^{\pi\bullet}GG]^+$, and the $\sigma_\alpha$ radicals $[Y\mathbf{G}^{\alpha\bullet}G]^+$ and $[YG\mathbf{G}^{\alpha\bullet}]^+$. The unpaired spin density of $[\mathbf{Y}^{\varepsilon\bullet}GG]^+$ is mainly at the ε-carbon atom (> 90%) and in the plane of the benzene ring. By contrast, the spin density of $[\mathbf{Y}^{\pi\bullet}GG]^+$ is delocalized over the $\pi$ orbitals of the carbon and oxygen atoms of the phenol unit (57.9%) but with a significant contribution (21.8%) from the amide oxygen that is located over the aromatic ring. Both $[Y\mathbf{G}^{\alpha\bullet}G]^+$ and $[YG\mathbf{G}^{\alpha\bullet}]^+$ have more than 50% of their spin density at the designated α-carbon atoms, while the remainder is delocalized over the amide residues (the second residue for $[Y\mathbf{G}^{\alpha\bullet}G]^+$ and the third for $[YG\mathbf{G}^{\alpha\bullet}]^+$). Therefore, these four radicals exhibit four different spin densities as expected.

## Potential Energy Profiles for Conversion of $[\mathbf{Y}^{\varepsilon\bullet}GG]^+$ into $[Y\mathbf{G}^{\alpha\bullet}G]^+$,$[YG\mathbf{G}^{\alpha\bullet}]^+$ and $[\mathbf{Y}^{\pi\bullet}GG]^+$

**Figure 4a** presents the PES for HAT from the glycyl residues to the $\sigma_\varepsilon$ radical center of $[\mathbf{Y}^{\varepsilon\bullet}GG]^+$, as determined at the UB3LYP/6-31++G(d,p) level of theory. All energies are relative to the best optimized structure for the highest energy isomer, $[\mathbf{Y}^{\varepsilon\bullet}GG]^+$, in which the radical is located at the ε-carbon atom of the tyrosine residue and the proton is located at the N-terminal nitrogen atom. Ion $[Y^{\alpha\bullet}G\mathbf{G}]^+$, stabilized by the presence of a strong donor ($NH_2$) and a powerful electron-withdrawing protonated carbonyl group both adjacent to the radical center, is at the global minimum, 38.5 kcal $mol^{-1}$ below the $[Y^{\varepsilon\bullet}GG]^+$ ion. Ion $[Y^{\alpha\bullet}G\mathbf{G}]^+$ does not interconvert easily into the other isomers and therefore, for the sake of clarity, was not included in Figure 4a.

A direct 1,8 hydrogen atom transfer from the α-carbon atom of the central glycine residue to the ε-carbon atom of the tyrosine residue has the highest energy barrier

(50.6 kcal mol$^{-1}$ relative to [Y$^{\varepsilon\bullet}$GG]$^+$). By contrast, a direct 1,11 HAT from the α-carbon atom of the terminal glycine residue ([YG**G**$^{\alpha\bullet}$]$^+$) to the ε-carbon atom of the tyrosine residue ([**Y**$^{\varepsilon\bullet}$GG]$^+$) has a substantially lower barrier (15.5 kcal mol$^{-1}$), indicating that conversion to [YG**G**$^{\alpha\bullet}$]$^+$ is facile. As the barrier to conversion between [YG**G**$^{\alpha\bullet}$]$^+$ and [Y**G**$^{\alpha\bullet}$G]$^+$ is expected to be approximately 36 kcal mol$^{-1}$ according to the isomerization barrier from [GG**G**$^{\alpha\bullet}$]$^+$ to [G**G**$^{\alpha\bullet}$G]$^+$, then conversion of [**Y**$^{\varepsilon\bullet}$GG]$^+$ into [Y**G**$^{\alpha\bullet}$G]$^+$ is more likely to follow the indirect route via [YG**G**$^{\alpha\bullet}$]$^+$.[43, 44] Furthermore, the loss of water from [GG**G**$^{\alpha\bullet}$]$^+$ was calculated to be slightly lower than that to rearrangement to [G**G**$^{\alpha\bullet}$G]$^+$ and similarly the loss of water is the base peak in the fragmentation of [YG**G**$^{\alpha\bullet}$]$^+$. All these calculations support the conclusion based on the experimental observations that [**Y**$^{\varepsilon\bullet}$GG]$^+$ converts to [YG**G**$^{\alpha\bullet}$]$^+$ prior to dissociation, but interconversion with [Y**G**$^{\alpha\bullet}$G]$^+$ does not occur.

Loss of ammonia from [Y**G**$^{\alpha\bullet}$G]$^+$ could occur either by (a) nucleophilic displacement by the phenol ring to form a phenonium ion as in the dissociation of protonated phenylalanine[45-48] or (b) by a 1,5 HAT from the β-carbon of the tyrosine side chain, followed by cleavage of the terminal N-$C_\alpha$ bond. The barrier to loss of $NH_3$ from protonated tyrosine via a phenonium ion has been calculated by DFT calculations at B3LYP/DZVP to be 31.9 kcal mol$^{-1}$ [49]; this compares with a barrier of 41.6 kcal mol$^{-1}$ for the rearrangement of [G**G**$^{\alpha\bullet}$G]$^+$ into [GG**G**$^{\alpha\bullet}$]$^+$.[44] Consequently, loss of ammonia by a charge-driven mechanism from [Y**G**$^{\alpha\bullet}$G]$^+$ is almost certainly favored over rearrangement to [GG**G**$^{\alpha\bullet}$]$^+$. The energy for the radical-driven process was more difficult to estimate so we calculated the transition state for the 1,5 HAT from the β-carbon of the tyrosine to α-carbon of the central residue and obtained a barrier of 28.2 kcal mol$^{-1}$. This is the rate-determining barrier as the energy of the products of dissociation was calculated to be 5.9 kcal mol$^{-1}$ below this transition state. Hence it appears that ammonia loss from [Y**G**$^{\alpha\bullet}$G]$^+$ is probably radical-driven.

Finally, conversion of the $[\mathbf{Y}^{\varepsilon\bullet}GG]^+$ ion into the π-radical $[\mathbf{Y}^{\pi\bullet}GG]^+$ formally occurs by proton migration from the N-terminal amino group to the radical center. The crucial barrier to this multistep process has a barrier of 24.4 kcal $mol^{-1}$ and clearly is energetically not competitive with the 1,11 HAT required to convert ion $[\mathbf{Y}^{\varepsilon\bullet}GG]^+$ into $[YG\mathbf{G}^{\alpha\bullet}]^+$. Although the direct migration conversion of $[\mathbf{Y}^{\varepsilon\bullet}GG]^+$ to phenoxy radical $[\mathbf{Y}^{O\bullet}GG]^+$ is energetically highly unfavorable (39.7 kcal $mol^{-1}$), direct 1,13 HAT pathway from $[YG\mathbf{G}^{\alpha\bullet}]^+$ to the $[\mathbf{Y}^{O\bullet}GG]^+$ (30.1kcal/mol) which subsequently results in facile formation of ion $[M-106]^{\bullet+}$ is possible.[25, 26] Consistent with the prior analysis, RRKM calculations (**Figure 4b**) confirm that the rate constant for conversion of $[\mathbf{Y}^{\varepsilon\bullet}GG]^+$ into $[YG\mathbf{G}^{\alpha\bullet}]^+$ is several orders of magnitude higher than those for formation of $[\mathbf{Y}^{\pi\bullet}GG]^+$ and $[Y\mathbf{G}^{\alpha\bullet}G]^+$ at low internal energy.

## Effect of substitution on the central residue

**Figure 5** displays the CID spectra of $[\mathbf{Y}^{\varepsilon\bullet}A_{\alpha CH3}G]^+$, $[YA_{\alpha CH3}\mathbf{G}^{\alpha\bullet}]^+$ and $[\mathbf{Y}^{\varepsilon\bullet}G_{d2}G]^+$, radical cations. Here the central glycyl residue has been replaced by an α-methylalanine residue or a α-deuterated glycyl residue; the former eliminates the possibility of forming an α-carbon–centered radical intermediate at this residue. The fragmentation patterns of $[\mathbf{Y}^{\varepsilon\bullet}A_{\alpha CH3}G]^+$ and $[YA_{\alpha CH3}\mathbf{G}^{\alpha\bullet}]^+$ are again almost identical supporting the hypothesis that direct radical migration occurs, rather than stepwise passage through an intermediate with the radical centered on the middle glycine residue. Similarly, no deuterium atoms from the deuterated radical cation $[\mathbf{Y}^{\varepsilon\bullet}G_{d2}G]^+$ were involved in the formation of the $b_2^+$ product, implying no role for the α-hydrogen atoms of the middle glycine residue in either the isomerization or fragmentation processes.

# CONCLUSION

The $[\mathbf{Y}^{\varepsilon\bullet}GG]^+$ radical cation, created by loss of $I^\bullet$ from protonated 3-iodotyrosylglycylglycine, has an identical fragmentation pattern to that of the $[YG\mathbf{G}^{\alpha\bullet}]^+$ ion, created by loss of isobutene from $[YGL]^{\bullet+}$. The $[YG\mathbf{G}^{\alpha\bullet}]^+$ ion is calculated to be 28.7 kcal $mol^{-1}$ lower in energy than $[\mathbf{Y}^{\varepsilon\bullet}GG]^+$ and, as the barrier to conversion by hydrogen atom transfer is only 15.5 kcal $mol^{-1}$ above $[\mathbf{Y}^{\varepsilon\bullet}GG]^+$, then we conclude that rearrangement occurs prior to dissociation. By comparison with calculations on $[GG\mathbf{G}^{\alpha\bullet}]^+$, the barrier to the dominant fragmentation channel of $[YG\mathbf{G}^{\alpha\bullet}]^+$, the loss of water, is estimated to be 32.5 kcal $mol^{-1}$, ~11 kcal $mol^{-1}$ less than for rearrangement back to $[\mathbf{Y}^{\varepsilon\bullet}GG]^+$. Also, $[YG\mathbf{G}^{\alpha\bullet}]^+$ and $[Y\mathbf{G}^{\alpha\bullet}G]^+$ gave different fragmentation products and the barrier to isomerization between these two ions (estimated to be 35.8 kcal $mol^{-1}$ above $[Y\mathbf{G}^{\alpha\bullet}G]^+$) is higher than those to dissociations for both ions.

# ACKNOWLEDGMENTS

This study was supported by the Hong Kong Research Grants Council (project nos. HKU 701611P and HKU 701613P), Hong Kong Special Administrative Region, China. Cheuk-Kuen Lai and Xiaoyan Mu thank the Hong Kong RGC for supporting their studentships. We thank Dr. Song Tao, and Mr. Shen Qing for technical assistance with the preliminary DFT calculations and experiments.

# REFERENCES


1 J. S. Brodbelt, *Chem. Soc. Rev.*, 2014, **43**, 2757-2783.

2 H. B. Oh, B. Moon, *Mass Spectrom. Rev.*, 2014, DOI: 10.1002/mas.21426.

3 F. Turecek, R. R. Julian, *Chem. Rev.*, 2013, **113**, 6691-6733.

4 I. K. Chu, J. Laskin, *Eur. J. Mass Spectrom.*, 2011, **17**, 543-556.

5 D. L. Marshall, C. S. Hansen, A. J. Trevitt, H. B. Oh, S. J. Blanksby, *Phys. Chem. Chem. Phys.*, 2014, **16**, 4871-4879.

6 S. Wee, R. A. J. O'Hair, W. D. McFadyen, *Int. J. Mass Spectrom.*, 2004, **234**, 101-122.

7 A. C. Hopkinson, *Mass Spectrom. Rev.*, 2009, **28**, 655-671.

8 M. Schafer, M. Drayss, A. Springer, P. Zacharias, K. Meerholz, *Eur. J. Org. Chem.*, 2007, 5162-5174.

9 F. Turecek, *Mass Spectrom. Rev.*, 2007, **26**, 563-582.

10 D. C. M. Ng, T. Song, S. O. Siu, C. K. Siu, J. Laskin, I. K. Chu, *J. Phys. Chem. B*, 2010, **114**, 2270-2280.

11 J. F. Zhao, C. M. D. Ng, I. K. Chu, K. W. M. Siu, A. C. Hopkinson, *Phys. Chem. Chem. Phys.*, 2009, **11**, 7629-7639.

12 J. F. Zhao, T. Song, M. J. Xu, Q. Quan, K. W. M. Siu, A. C. Hopkinson, I. K. Chu, *Phys. Chem. Chem. Phys.*, 2012, **14**, 8723-8731.

13 I. K. Chu, C. F. Rodriguez, A. C. Hopkinson, K. W. Siu, T. C. Lau, *J. Am. Soc. Mass Spectrom.*, 2001, **12**, 1114-1119.

14 I. K. Chu, J. Zhao, M. Xu, S. O. Siu, A. C. Hopkinson, K. W. M. Siu, *J. Am. Chem. Soc.*, 2008, **130**, 7862-7872.

15 E. R. Knudsen, R. R. Julian, *Int. J. Mass Spectrom.*, 2010, **294**, 83-87.

16 S. Osburn, R. A. J. O'Hair, V. Ryzhov, *Int. J. Mass Spectrom.*, 2012, **316**, 133-139.

17 V. Ryzhov, A. K. Y. Lam, R. A. J. O'Hair, *J. Am. Soc. Mass Spectrom.*, 2009, **20**, 985-995.

18 G. K. Yeh, Q. Y. Sun, C. Meneses, R. R. Julian, *J. Am. Soc. Mass Spectrom.*, 2009, **20**, 385-393.

19 J. K. Diedrich, R. R. Julian, *J. Am. Chem. Soc.*, 2008, **130**, 12212-12213.

20 J. K. Diedrich, R. R. Julian, *Anal. Chem.*, 2011, **83**, 6818-6826.

21 A. Agarwal, J. K. Diedrich, R. R. Julian, *Anal. Chem.*, 2011, **83**, 6455-6458.

22 Z. Liu, R. R. Julian, *J. Am. Soc. Mass Spectrom.*, 2009, **20**, 965-971.

23 T. Ly, R. R. Julian, *J. Am. Chem. Soc.*, 2008, **130**, 351-358.

24 C. K. Siu, Y. Ke, Y. Guo, A. C. Hopkinson, K. W. M. Siu, *Phys. Chem. Chem. Phys.*, 2008, **10**, 5908-5918.

25 I. K. Chu, C. F. Rodriquez, T. C. Lau, A. C. Hopkinson, K. W. M. Siu, *J. Phys. Chem. B*, 2000, **104**, 3393-3397.

26 C. K. Barlow, W. D. McFadyen, R. A. J. O'Hair, *J. Am. Chem. Soc.*, 2005, **127**, 6109-6115.

27 C. K. Lai, D. C. M. Ng, H. F. Pang, J. C. Y. Le Blanc, J. W. Hager, D. C. Fang, A. S. C. Cheung, I. K. Chu, *Rapid Commun. Mass Spectrom.*, 2013, **27**, 1119-1127.

28 Q. Hao, T. Song, D. C. M. Ng, Q. Quan, C. K. Siu, I. K. Chu, *J. Phys. Chem. B*, 2012, **116**, 7627-7634.

29 T. Song, Q. Hao, C. H. Law, C. K. Siu, I. K. Chu, *J. Am. Soc. Mass Spectrom.*, 2012, **23**, 264-273.

30 W. C. Chan, P. D. White, *Fmoc solid phase peptide synthesis : a practical approach*, Oxford University Press, New York, 2000.

31 A. D. Becke, *J. Chem. Phys.*, 1993, **98**, 5648-5652.

32 T. Clark, J. Chandrasekhar, G. W. Spitznagel, P. V. Schleyer, *J. Comput. Chem.*, 1983, **4**, 294-301.

33 W. J. Hehre, R. Ditchfield, J. A. Pople, *J. Chem. Phys.*, 1972, **56**, 2257-2261.

34 *SPARTAN '04*, (2004) Wavefunction, Inc.

35 G. W. T. M. J. Frisch, H. B. Schlegel, G. E. Scuseria, M. A. Robb, J. R. Cheeseman, J. A. Montgomery, Jr., T. Vreven, K. N. Kudin, J. C. Burant, J. M. Millam, S. S. Iyengar, J. Tomasi, V. Barone, B. Mennucci, M. Cossi, G. Scalmani, N. Rega, G. A. Petersson, H. Nakatsuji, M. Hada, M. Ehara, K. Toyota, R. Fukuda, J. Hasegawa, M. Ishida, T. Nakajima, Y. Honda, O. Kitao, H. Nakai, M. Klene, X. Li, J. E. Knox, H. P. Hratchian, J. B. Cross, V. Bakken, C. Adamo, J. Jaramillo, R. Gomperts, R. E. Stratmann, O. Yazyev, A. J. Austin, R. Cammi, C. Pomelli, J. W. Ochterski, P. Y. Ayala, K. Morokuma, G. A. Voth, P. Salvador, J. J. Dannenberg, V. G. Zakrzewski, S. Dapprich, A. D. Daniels, M. C. Strain, O. Farkas, D. K. Malick, A. D. Rabuck, K. Raghavachari, J. B. Foresman, J. V. Ortiz, Q. Cui, A. G. Baboul, S. Clifford, J. Cioslowski, B. B. Stefanov, G. Liu, A. Liashenko, P. Piskorz, I. Komaromi, R. L. Martin, D. J. Fox, T. Keith, M. A. Al-Laham, C. Y. Peng, A. Nanayakkara, M. Challacombe, P. M. W. Gill, B. Johnson, W. Chen, M. W. Wong, C. Gonzalez, and J. A. Pople, *Gaussian 03, revision C.02*, (2004) Gaussian, Inc., Wallingford, CT.

36 T. Baer, P. M. Mayer, *J. Am. Soc. Mass Spectrom.*, 1997, **8**, 103-115.

37 T. Beyer, D. F. Swinehar, *Commun. Acm.*, 1973, **16**, 379-379.

38 T. Song, D. C. M. Ng, Q. Quan, C. K. Siu, I. K. Chu, *Chem.-Asian J.*, 2011, **6**, 888-898.

39 T. Ly, R. R. Julian, *J. Am. Soc. Mass Spectrom.*, 2009, **20**, 1148-1158.

40 X. Zhang, R. R. Julian, *J. Am. Soc. Mass Spectrom.*, 2013, **24**, 524-533.

41 J. K. C. Lau, J. F. Zhao, K. W. M. Siu, A. C. Hopkinson, *Int. J. Mass Spectrom.*, 2012, **316**, 268-272.

42 U. H. Verkerk, J. F. Zhao, M. J. Van Stipdonk, B. J. Bythell, J. Oomens, A. C. Hopkinson, K. M. Siu, *J. Phys. Chem. A*, 2011, **115**, 6683-6687.

43 I. K. Chu, J. Zhao, M. J. Xu, S. O. Siu, A. C. Hopkinson, K. W. M. Siu, *J. Am. Chem. Soc.*, 2008, **130**, 7862-7872.

44 C. K. Siu, J. Zhao, J. Laskin, I. K. Chu, A. C. Hopkinson, K. W. Siu, *J. Am. Soc. Mass Spectrom.*, 2009, **20**, 996-1005.

45 N. N. Dookeran, T. Yalcin, A. G. Harrison, *J. Mass Spectrom.*, 1996, **31**, 500-508.

46 H. Lioe, R. A. J. O'Hair, *Org. Biomol. Chem.*, 2005, **3**, 3618-3628.

47 F. Rogalewicz, Y. Hoppilliard, G. Ohanessian, *Int. J. Mass Spectrom.*, 2000, **195**, 565-590.

48 T. Shoeib, A. Cunje, A. C. Hopkinson, K. W. M. Siu, *J. Am. Soc. Mass Spectrom.*, 2002, **13**, 408-416.

49 J. F. Zhao, T. Shoeib, K. W. M. Siu, A. C. Hopkinson, *Int. J. Mass Spectrom.*, 2006, **255**, 265-278.